Inorganica Chimica Acta 438 (2015) 203–207

Contents lists available at ScienceDirect

Inorganica Chimica Acta

journal homepage: www.elsevier.com/locate/ica

Computational study of the structure, bonding and reactivity of selected helical metallocenes

U.E. Cázares-Larios, U.G. Reyes-Leaño, P.A. Castillo-López, K. Pineda-Urbina *, Z. Gómez-Sandoval *

Facultad de Ciencias Químicas, Universidad de Colima, Carretera Colima-Coquimatlán km. 9, Coquimatlán, Colima Col. C.P. 28400, Mexico

ARTICLE INFO

Article history:
Received 30 July 2015
Received in revised form 19 September 2015
Accepted 21 September 2015
Available online 30 September 2015

Keywords:
DFT
Fukui function
EDA
Metallocenes
Helical ligands

ABSTRACT

A series of helicoid metallocenes structures were studied *in silico* under the DFT framework. Their reactivity was explored by the dual Fukui function. An energy decomposition analysis was performed in order to gain insight into the interaction between the helix-like ligand and the metallic nuclei. Helical cobaltocene was highlighted as an interesting synthetic target through its peculiar response to ionization as well as its interaction and preparation energies.

1. Introduction

Kealy and Pauson introduced the ferrocene to the world over 60 years ago [1]. This molecule served as the cornerstone that opened up a whole new group of molecular systems for study, the metallocenes. Metallocenes have found their place in science with applications in asymmetrical catalysis, polymerization, antitumoral agents and malaria treatment, besides the basic contributions from studying their peculiar structure and bonding.

Within the metallocenes, the helical ferrocene reported by Katz and Pesti in 1982 stands out as a very interesting synthesized structure [2]. This molecule contains a helical organic ligand formed by two cyclopentadiene rings linked by five fused benzene rings, bound on both ends to an iron atom. The resulting structure presents a conjugated chiral system which could display chiroptical activity and interesting electrical properties, besides the helix-like pattern of interest itself as it's recurrently found in proteins, nucleic acids, polysaccharides and such [3–7]. There has been previous attempts to expand on this helicoid ferrocene like the proposal of a new structure with a similar but longer ligand, for example. Despite all this, there is surprisingly little information about this particular type of metallocene [8]. Due to the nature of the metal–ligand and ligand–ligand interactions, the electronic properties of a helical metallocene could vary just by changing the metal center, associated with the coordination sphere geometry and oxidation state. Hence, a group of helical metallocenes using Katz and Pesti's ligand, along with the metals of the fourth period is proposed. Their structures and reactivity are compared to the available data from experimental sources and previous theoretical studies [9–11].

2. Computational details

Full structure optimizations, without symmetry constraints, were performed with the generalized gradient approximation (GGA) employing the exchange–correlation functional proposed by Becke and Perdew (BP86) [12,13]. All electrons were treated explicitly using the triple zeta valence plus polarization (def2-TZVP) basis set for all atoms as they are implemented in the *ORCA* code [14–16]. In order to verify the optimized minima on the potential energy surface, a frequency analysis was performed. Having established the lowest energy stationary points for each molecule, a set of reactivity properties was calculated assuming a vertical ionization approximation. The same stationary points were used to calculate the Fukui functions employing ADPT with the BP86 functional, DZVP basis set and GEN-A2* auxiliary basis set on the *deMon2k* software [17–22]. EDA calculations were performed on the Amsterdam Density Functional (ADF) software [23–26]. They all used the BP86 functional and the TZ2P STO basis set. The ZORA approximation was employed in order to include relativistic effects. The images were rendered by the molecular

---

* Corresponding authors.
E-mail addresses: kpineda@ucol.mx (K. Pineda-Urbina), zgomez@ucol.mx (Z. Gómez-Sandoval).

http://dx.doi.org/10.1016/j.ica.2015.09.017
0020-1693/

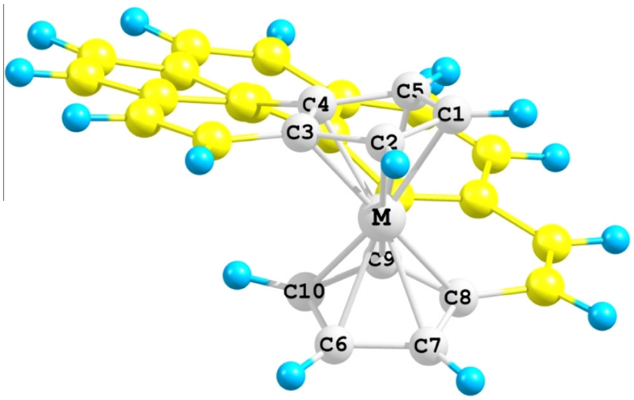

Fig. 1. Helical metallocene general structure.

Table 1
Helical metallocene energy gap.

Metal	Multiplicity	HLG (kcal/mol)
Sc	2	11.39
Ti	1	15.25
V	4	26.07
Cr	1	17.28
Mn	2	24.35
Fe	1	33.29
Co	2	13.30
Ni	3	11.30
Zn	1	53.34

visualizer *Sinapsis*, except for Fig. 1, which was done with ChemCraft [27,28].

3. Results and discussion

A procedural exploration of different multiplicities was done for each proposed metallocene. Every helical system was optimized using four different spin multiplicities; 1, 3, 5 and 7 for compounds with an even number of electrons and 2, 4, 6 and 8 for the ones with an odd number of electrons. These results were used to select a single structure for each helical metallocene, based on two structural stability criterion: the lowest total energy and the largest HOMO–LUMO gap or SOMO–LUMO gap (henceforth called HLG indistinctively). They are attached as Supplementary material. The metallocenes' selected structures fulfilled both criteria and their multiplicity and HLG are listed on Table 1.

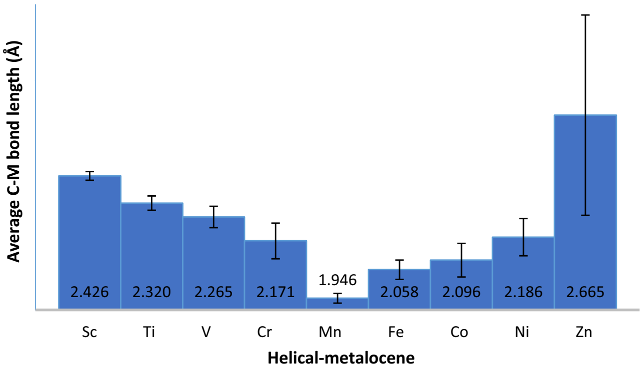

Fig. 2. Average C–M bond length in angstrom of each helical metallocene with their respective standard deviation.

The HLG calculated for some of the selected structures is small – probably as a consequence of their extended conjugation – which certainly sets them up as challenging synthetic targets. However, there has been successful experimentations on systems with HLG of similar magnitude and there are at least two established approaches for their synthesis [29–31]. Moreover, the HLGs calculated for the helical vanadocene and helical manganocene are closer to the HLG calculated for the experimentally available helical ferrocene suggesting that a similar approach to their synthesis is not out of the question.

The bond lengths between the metal and the Cp rings were analyzed for the selected structures and are listed on Table 2 (use Fig. 1 for reference).

Theoretical bond lengths from the helical ferrocene concord nicely with the experimental data from [32]. The deformation of the helical zincocene's structure is evident from looking at the rather large standard deviation of its C–Zn bond lengths. There is an evident trend in the bond lengths, where the helical manganocene system has the shortest average C–M bond length and this number gets larger as you move farther away from manganese on the periodic table (Fig. 2).

There is a direct correlation between the reported effective ionic radii of the metals and the average bond length of the metallocenes (Fig. 3) [33]. Scandium was omitted from the effective ionic radii graph as there is no data available for its oxidation state 2+.

A first approach towards the characterization of the proposed helical metallocenes' local reactivity was done with the Fukui function. The Fukui function is a tool which predicts the change of the electronic density due to a change in the number of electrons of a system. Formally, the Fukui function is the derivative of the

Table 2
Metallocene bond lengths, average bond lengths and standard deviations.

Bond	Metal									
	Sc	Ti	V	Cr	Mn	Fe*	Fe	Co	Ni	Zn
C1–M	2.446	2.328	2.290	2.168	1.934	2.070	2.073	2.088	2.131	2.582
C2–M	2.399	2.320	2.306	2.240	1.931	2.079	2.090	2.116	2.230	2.028
C3–M	2.429	2.365	2.301	2.258	1.982	2.087	2.098	2.210	2.301	2.554
C4–M	2.415	2.301	2.209	2.115	1.938	2.008	2.005	2.036	2.171	3.059
C5–M	2.440	2.283	2.220	2.076	1.945	2.017	2.021	2.029	2.095	3.101
C6–M	2.449	2.328	2.290	2.167	1.934	2.055	2.073	2.087	2.130	2.582
C7–M	2.401	2.320	2.305	2.240	1.931	2.084	2.092	2.115	2.230	2.028
C8–M	2.429	2.366	2.301	2.257	1.982	2.104	2.101	2.210	2.302	2.554
C9–M	2.414	2.302	2.210	2.115	1.938	2.007	2.006	2.036	2.172	3.059
C10–M	2.441	2.283	2.220	2.076	1.946	2.013	2.020	2.029	2.096	3.101
$\bar{X}$	2.426	2.319	2.265	2.171	1.946	2.052	2.057	2.095	2.185	2.664
σ	0.017	0.028	0.042	0.070	0.019	0.036	0.038	0.066	0.073	0.393

* Experimental data from [32].